

JUNO Status and Physics Potential [†]

Livia Ludhova ^{1,2}  on behalf of the JUNO Collaboration

¹ Nuclear Physics Institute IKP-2, Forschungszentrum Jülich GmbH, Wilhelm-Johnen-Straße, 52428 Jülich, Germany; l.ludhova@fz-juelich.de

² Physics Institute III B, RWTH Aachen University, Otto-Blumenthal-Straße, 52074 Aachen, Germany

[†] Presented at the 23rd International Workshop on Neutrinos from Accelerators, Salt Lake City, UT, USA, 30–31 July 2022.

Abstract: The Jiangmen Underground Neutrino Observatory (JUNO) is a neutrino experiment under construction in an underground laboratory with a 650 m rock overburden near Jiangmen in southern China. The detector's main component will be 20 kton of liquid scintillator held in a spherical acrylic vessel. The experiment is designed for the determination of neutrino mass ordering, one of the key open questions in neutrino physics. This measurement will be based on observations of the vacuum oscillation pattern of antineutrinos from two nuclear power plants at a baseline of 53 km. The estimated sensitivity is 3σ in about six years with 26.6 GW_{th} of reactor power. A key ingredient for the success is an excellent and extremely challenging energy resolution of 3% at 1 MeV. The light produced by the scintillator will be seen by 17,612 large twenty-inch PMTs and 25,600 small three-inch PMTs. The OSIRIS detector will monitor the radio purity of the liquid scintillator during the months-long filling process of the main detector. The unoscillated antineutrino spectrum from one reactor core will be measured with unprecedented precision by the Taishan Antineutrino Observatory (TAO), located at a baseline of about 30 m. JUNO is expected to substantially improve the precision of $\sin^2 2\theta_{12}$, Δm_{21}^2 , and Δm_{31}^2 neutrino oscillation parameters. Astrophysical measurements of solar, geo-, supernova, DSNB, and atmospheric neutrinos, as well as searching for proton decay and dark matter, are integral parts of the vast JUNO physics program. This contribution reviews the physics goals and current status of the JUNO project.

Keywords: neutrino detector; liquid scintillator; neutrino oscillations; reactor neutrinos; neutrino mass ordering; solar neutrinos; geoneutrinos; supernovae neutrinos; DSNB; atmospheric neutrinos



Citation: Ludhova, L., on behalf of the JUNO Collaboration JUNO Status and Physics Potential. *Phys. Sci. Forum* **2023**, *8*, 25. <https://doi.org/10.3390/psf2023008025>

Academic Editor: Yue Zhao

Published: 28 July 2023



Copyright: © 2023 by the author. Licensee MDPI, Basel, Switzerland. This article is an open access article distributed under the terms and conditions of the Creative Commons Attribution (CC BY) license (<https://creativecommons.org/licenses/by/4.0/>).

1. Introduction

The Jiangmen Underground Neutrino Observatory (JUNO) is a 20 kton liquid scintillator (LS) detector currently under construction in Jiangmen, Guangdong province, South China [1]. A dedicated underground laboratory with a 650 m rock overburden has been built. The detector installation is expected to be finished by the end of 2023. The main goal is the determination of neutrino mass ordering (NMO) via measurement of reactor electron antineutrinos from two adjacent nuclear power plants at a baseline of 53 km each, as shown in Figure 1 (left). With a total reactor thermal power of 26.6 GW_{th} (six cores at Yangjiang and two cores at Taishan), the expected sensitivity of JUNO to NMO is 3σ in about six years. Thanks to the unprecedented size and energy resolution of the detector, JUNO has a vast potential in many other areas of neutrino and astroparticle physics. The JUNO Collaboration was established in 2014, and currently comprises 76 institutions from eighteen countries and nearly 700 collaborators in all.

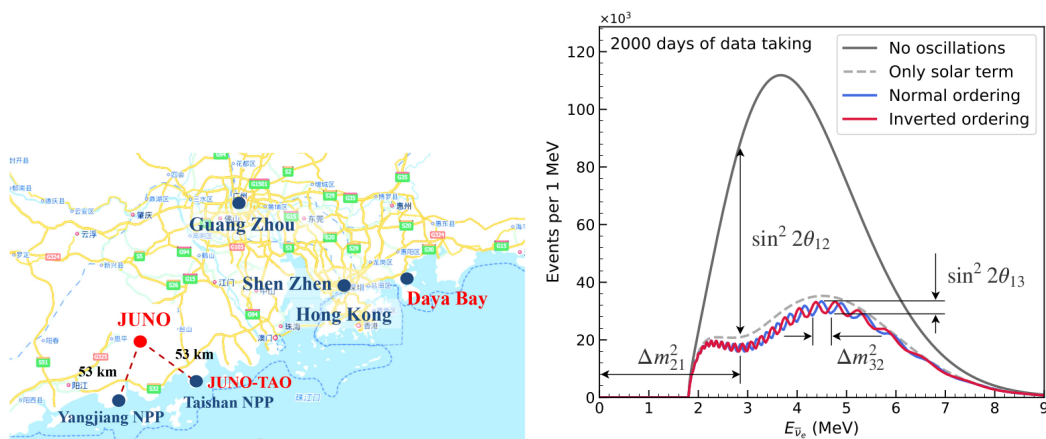


Figure 1. Left: The Jiangmen Underground Observatory (JUNO) is located in Guangdong province, South China. The locations of the Yangjiang and Taishan nuclear power plants (NPPs) are shown as well. Right: the expected JUNO reactor antineutrino energy spectrum after 2000 days of data taking in scenarios assuming no oscillations (solid black), oscillations under normal ordering (solid blue), and oscillations under inverted ordering (solid red). Features that depend on the four oscillation parameters are highlighted. From [2].

The Main Goal Determines the Design

It is presently not known whether the neutrino mass eigenstate with the highest fraction of electron flavour is the lightest (normal ordering, NO) or the heaviest (inverted ordering, IO). JUNO will determine which of these two scenarios is realized in nature by detecting reactor electron antineutrinos. Nuclear reactors are the strongest human-made source of electron flavour antineutrinos with energy extending to up to about 10 MeV. JUNO will detect reactor antineutrinos via inverse beta decay interaction on protons (IBD):



The IBD interaction has a kinematic threshold of 1.806 MeV and its cross-section is known with sub-percent precision [3]. Thanks to the interplay between the energy dependencies of the emitted reactor neutrinos (decreasing with energy) and the IBD cross-section (increasing with energy), the spectrum of detected reactor antineutrinos without oscillations peaks between 3 and 4 MeV. Because the IBD is a charged current interaction, it is only sensitive to electron flavour antineutrinos. Thus, the electron flavour survival probability P_{ee} at a certain baseline determines the shape of the measured energy spectrum of antineutrinos. The oscillation pattern is composed of two components: the “slow solar oscillation” pattern depends on the solar oscillation parameters $\sin^2 2\theta_{12}$ and Δm^2_{21} , while the “fast atmospheric oscillation” depends on $\sin^2 2\theta_{13}$ and Δm^2_{31} . Because Δm^2_{31} has a different sign as well as a different absolute value in the NO and IO scenarios, the final oscillation pattern expected in JUNO in the two scenarios is different, as shown in Figure 1 (right). This method [4] based on the vacuum oscillation of antineutrinos is complementary to the method based on the effects of matter on long baseline oscillations of GeV-scale atmospheric and accelerator neutrinos, which additionally depends on the CP-violation phase and the θ_{23} mixing angle.

2. JUNO in a Nutshell

In order to resolve the fast oscillation pattern, statistics of about 100,000 IBD events at a 53 km baseline are needed, which requires a large amount of thermal power from nuclear power plants (26.6 GW_{th}) and a large target mass (20 kton of LS). Additionally, JUNO must achieve an unprecedented energy resolution of about 3% at 1 MeV, better than 1% understanding of the intrinsically nonlinear energy scale of the LS, as well as a very precise knowledge of the shape of the unoscillated reactor spectrum. The cosmogenic

background is strongly reduced thanks to 1800 m water equivalent of the rock overburden. A complex strategy to minimize the radioactivity levels of the LS as well as of all the construction materials has been developed [5]. The stability of all the components in the time span of about a decade must be guaranteed. In order to maintain the stochastic terms in the energy resolution at sufficient levels, the LS needs to have a high light yield (about 10^4 photons/MeV) and an excellent transparency ($\lambda_{\text{att}} > 20$ m at 430 nm); the detector's geometrical coverage with photomultipliers (PMTs) will be 78%, and the PMT combined collection and quantum efficiency will be about 30%. The composition of the JUNO LS has been optimized by using a Daya Bay antineutrino detector [6]. The systematic effects of the energy scale will be kept under control with an extensive calibration campaign [7] and using a double calorimetry system of the large twenty-inch and the small three-inch PMTs. The Taishan Antineutrino Observatory (TAO) [8], a satellite detector that is a part of JUNO, will be built at a distance of 30 m from the Taishan-1 reactor core with an energy resolution below 2% at the energy of interest. TAO will measure the reactor's unoscillated antineutrino energy spectrum with unprecedented precision.

Detector Design and Status

The civil construction of the the JUNO site was completed in December 2021. The underground experimental hall is connected to the surface by a 1266 m slope tunnel and a 564 m vertical shaft. A sketch of the JUNO detector is shown in Figure 2 (left). The Central Detector (CD) will be filled with 20 kton of LS contained in a spherical acrylic vessel with a diameter of 35.4 m. The acrylic panels of the CD detector are being mounted from an installation platform, the construction of which was completed in May 2022. The CD is supported by a stainless steel support structure that was finished in June 2022, as shown in Figure 2 (right). The PMTs with their front-end electronics will be mounted on the support structure. The Water Cherenkov Detector (WCD) will consist of 35 kton of ultra-pure water surrounding the CD. The WCD will serve like an active veto of cosmic muons with an efficiency of $>99.5\%$ as well as a passive shield against the external background neutrons and γ s. The Top Tracker (TT) composed of an array of plastic scintillator plates will cover 60% of the area above the WCD. The direction of muons crossing the TT will be measured with an angular resolution of 0.2° , corresponding to 20 cm at the bottom of the CD.

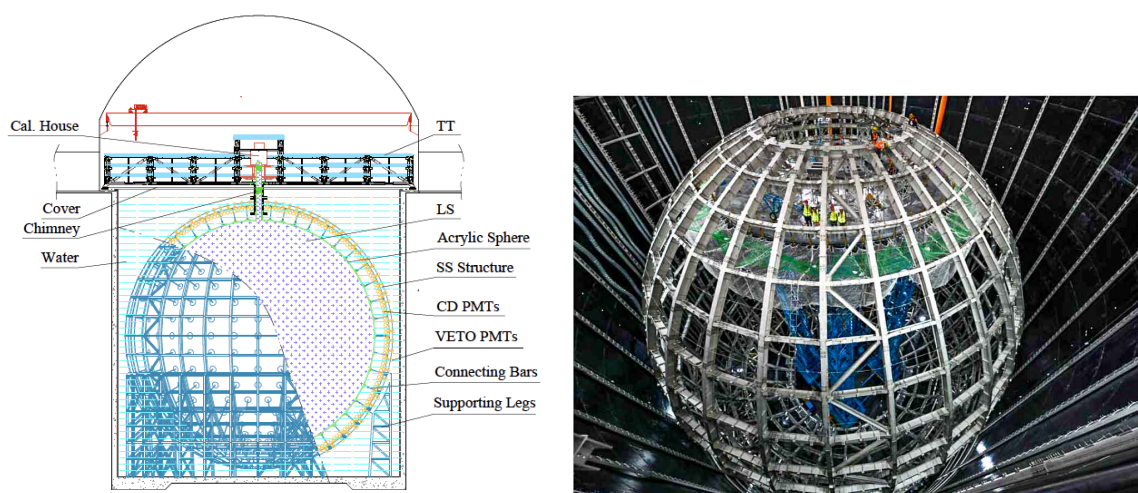


Figure 2. Left: sketch of the JUNO detector indicating the main subsystems. From [1]. Right: support structure of the central detector and the installation platform with workers (photo from June 2022).

The scintillation light will be detected by arrays of 17,612 twenty-inch Large PMTs (LPMTs) and 25,600 three-inch Small PMTs (SPMTs). The LPMTs are of two kinds, about one third from Hamamatsu and the rest multi-channel (MCP) PMTs produced by NNVT. All LPMTs have been produced, tested, and instrumented with waterproof potting. The total coverage of the LPMTs is 75%. SPMTs installed in the spaces between the LPMTs will provide an additional 3% geometrical coverage and a complementary set of sensors for the same events as for the LPMTs. The WCD will be equipped with 2400 LMPTs.

The LS is based on Linear Alkyl Benzene (LAB) as a solvent with an addition of 3 g/L of 2,5-diphenyloxazole (PPO) and 15 mg/L of 1,4-bis(2-methylstyryl) benzene (bis-MSB) as wavelength shifters. In order to meet the stringent LS radio purity requirement, e.g., a U/Th concentration of 10^{-15} g/g (for NMO determination) and 10^{-17} g/g (for solar neutrino measurement), a scintillator processing system has been built. The LS system includes four purification stages (Al_2O_3 column, distillation, water extraction, and steam stripping) as well as storage and mixing tanks. The achieved level of LS radiopurity will be tested in the 20 ton OSIRIS (Online Scintillator Internal Radioactivity Investigation System) detector [9]. After a successful test of each purification batch, the LS will be filled in the CD.

The further key steps towards completion of the JUNO detector are the finalisation of the acrylic vessel's construction, PMT installation, completion of the LS purification plants and OSIRIS pre-detector, and finally the six-months process of filling the LS in the CD. The satellite TAO detector will be a 2.8 ton Gd-loaded LS detector cooled to -50° , and will have more than 94% geometrical coverage achieved with 10 m^2 of SiPM with 50% detection efficiency. The TAO prototype will soon be completed at IHEP in China.

3. Physics Potential

With its large target mass and an extraordinary performance, JUNO will have a vast potential to precisely test neutrino properties and to use neutrinos as messengers to study various astronomical objects. Each day, JUNO will detect about 60 reactor neutrinos, thousands of solar neutrinos, and a few atmospheric neutrinos. Each year, JUNO will measure about 400 geoneutrinos and a few events from the Diffuse Supernovae Background (DSNB) are expected. In case of a core collapse supernova (CCSN) at a distance of 10 kpc, thousands of events will be detected on a time scale of only a few seconds. Additionally, JUNO will search for signs of a new physics by testing hypotheses of proton decay, neutrino magnetic moment, sterile neutrinos, nonstandard neutrino interactions, Lorentz invariance violation, and more.

3.1. Neutrino Mass Ordering and Neutrino Oscillation Parameters

Reactor antineutrinos are detected by the IBD interaction, as discussed above (Equation (1)), during which an electron flavour antineutrino is captured on a free proton (hydrogen nucleus), producing a positron and a neutron. The positron first deposits its kinetic energy and then it annihilates, producing two gammas with $E_\gamma = 0.511$ MeV each. These two processes cannot be distinguished and lead to the creation of a *prompt event*. The energy of the antineutrino is mostly transferred to the positron; thus, the visible energy of a prompt event $E_{vis}^{e^+}$ can be directly connected with the antineutrino energy $E_{\bar{\nu}_e}$:

$$E_{vis}^{e^+} = 2 \cdot E_\gamma + E_{\bar{\nu}_e} - 1.806 \text{ MeV} = E_{\bar{\nu}_e} - 0.784 \text{ MeV}. \quad (2)$$

The neutron is first thermalised and then captured on hydrogen ($\tau \sim 200 \mu\text{s}$). The capture is accompanied by a 2.2 MeV gamma, a *delayed event*. The IBD represents a golden channel to detect antineutrinos while significantly suppressing backgrounds by exploiting the prompt-delayed space and time coincidence.

The original evaluation of JUNO’s sensitivity to NMO [10] was recently updated and presented at the Neutrino 2022 conference. With respect to the original estimate, only two (not four) Taishan reactor cores will be built in near future, meaning that the total reactor power at 53 km baseline will be 26.6 GW_{th}. The JUNO experimental hall will be 60 m shallower, causing a 30% increase in the residual muon flux. These negative effects are compensated for by several positive developments. The estimated energy resolution is improved from 3% to 2.9% at 1 MeV due to various effects, including an increase in the photon detection efficiency resulting from the mass PMT testing [11], a new PMT optical model [12], and an updated CD geometry. An improved reactor spectral shape uncertainty will be achieved thanks to the construction of TAO [8]. An improved muon veto strategy leads to the exposure after veto being increased from 83% to 91.6%. Additionally, the expected background rates and radio purity of the construction materials have been updated [5]. Furthermore, a new modelling of the LS properties and its nonlinearity has been achieved by building on the experience of the Daya Bay experiment. Overall, JUNO’s expected sensitivity in determining NMO with reactor antineutrinos is now 3σ after about six years with 26.6 GW_{th} of reactor power. The time evolution of this sensitivity to NMO for both NO and IO scenarios is shown in Figure 3 (left). By exploiting the dependency of the energy spectrum on neutrino oscillation parameters, as shown in Figure 1 (right), in six years the parameters sin² 2θ₁₂, Δm²₂₁, and Δm²₃₁ will be measured with precision better than 0.5% [2]. The expected time evolution of the precision of this measurement is shown in Figure 1 (right).

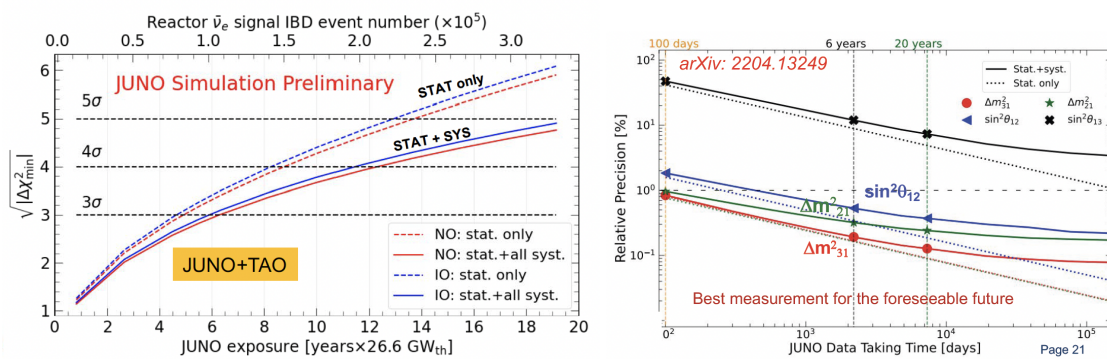


Figure 3. Sensitivity of JUNO. **Left:** sensitivity for determining neutrino mass ordering by exploiting the reference reactor spectrum of TAO. **Right:** sensitivity for precisely measuring neutrino oscillation parameters [2].

3.2. Solar Neutrinos

The sun is a strong natural source of MeV-scale neutrinos. Solar neutrinos are produced in the electron flavor (ν_e) during the process of nuclear fusion of hydrogen into helium in the core of the sun. The vast majority (about 99%) of solar energy comes from the so-called *pp* chain, producing *pp*, *pep*, ${}^7\text{Be}$, ${}^8\text{B}$, and *hep* neutrinos with distinct energy spectra. The remaining small fraction of solar energy is produced in the CNO cycle, in which fusion is catalysed by the presence of carbon, nitrogen, and oxygen. Detection of solar neutrinos provides key information about both the sun and the neutrino oscillations, particularly oscillations in dense solar matter.

Neutrinos of all flavours can be detected through the neutrino–electron elastic scattering (ES) process $\nu_{e,\mu,\tau} + e \rightarrow \nu_{e,\mu,\tau} + e$, in which neutrinos interact with the electrons present in the LS. In this process, a fraction of the neutrino energy is transferred to the electron, which is finally responsible for the generation of scintillation light in the detector. Thus, the electron recoil spectrum is continuous even in the case of mono-energetic neutrinos. The elastic scattering process has no threshold. The cross-section for ν_e scattering is about five times larger with respect to the $\nu_{\mu,\tau} - e$ scattering process. This is due to the fact that the latter proceeds only through neutral current (NC) interactions, while additional ν_e interac-

tions are possible via charged current (CC) interactions. This means that the detected rate of solar neutrinos measured through the ES process depends on the flavour composition of the incoming flux. It is impossible to distinguish the electrons scattered by solar neutrinos from the background components on an event-by-event basis. Therefore, solar neutrino signal is typically disentangled from the residual background through spectral fitting of selected events.

The sensitivity of JUNO to ^8B solar neutrinos, characterised by a low flux and an energy spectrum extending up to about 15 MeV, via the ES channel has been studied in [13]. A model independent approach to studying ^8B solar neutrinos by exploiting the roughly 200 tons of ^{13}C in the JUNO LS has recently been suggested in [14]. Here, in addition to the ES channel, CC and NC interactions on ^{13}C will be analyzed. CC interaction is sensitive only to the electron flavour neutrinos, while the NC interaction is sensitive to the overall flux independently of its flavour composition. The expected energy spectra of the ^8B solar neutrino signal and background components in this measurement are shown in Figure 4. The evaluated precision for determining the ^8B solar neutrino flux is 5%. Additionally, JUNO will measure the $\sin^2 2\theta_{12}$ and Δm_{21}^2 oscillation parameters with ^8B solar neutrinos.

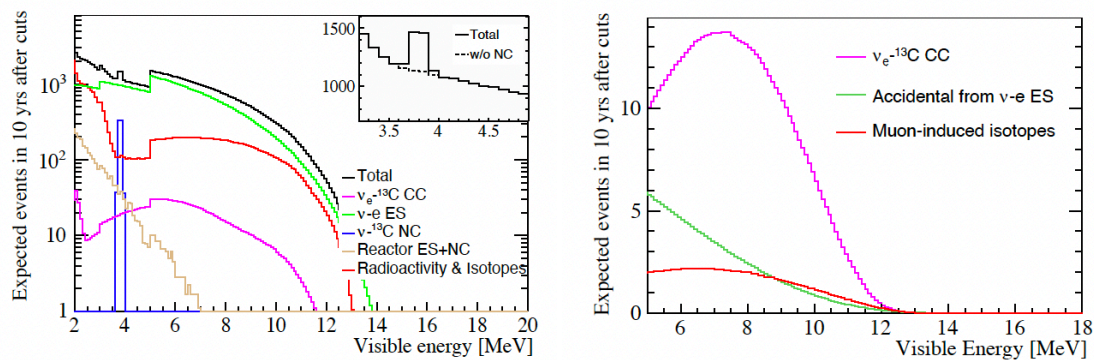


Figure 4. The energy spectra of ^8B solar neutrino signal and background components expected via measurement exploiting elastic scattering (ES) from electrons as well as CC and NC interactions on ^{13}C [14]. **Left:** plot representing the channel of single events. **Right:** plot representing the prompt signal of the delayed coincidence event characteristic for the CC interaction on ^{13}C .

The sensitivity of JUNO to ^7Be , pep , and CNO solar neutrinos will depend heavily on the achieved level of radio purity. Several radio purity scenarios were considered in a recent study [15], from the *Very Low background level* achieved by the Borexino experiment [16] up to the *High background* one (the minimum required for the NMO determination), as demonstrated in Figure 5 (left). For ^7Be neutrinos, JUNO will reach the current precision of 2.7% achieved by Borexino [17] after one year of data collection. For pep neutrinos, JUNO will improve on the current best result of 17% [17] after two years of data collection, except for the High background scenario, for which six years are needed. For the CNO neutrinos, the constraint on the rate of pep neutrinos in the spectral fit remains crucial, and can be achieved using existing data and theoretical assumptions [16]. However, JUNO will be able to detect CNO solar neutrinos without the ^{210}Bi constraint applied in the Borexino analysis [16,18], and will achieve 20% precision in two to four years, again with the exception of the High background scenario. Additionally, JUNO might be able to distinguish the ^{13}N and ^{15}O CNO components for the first time.

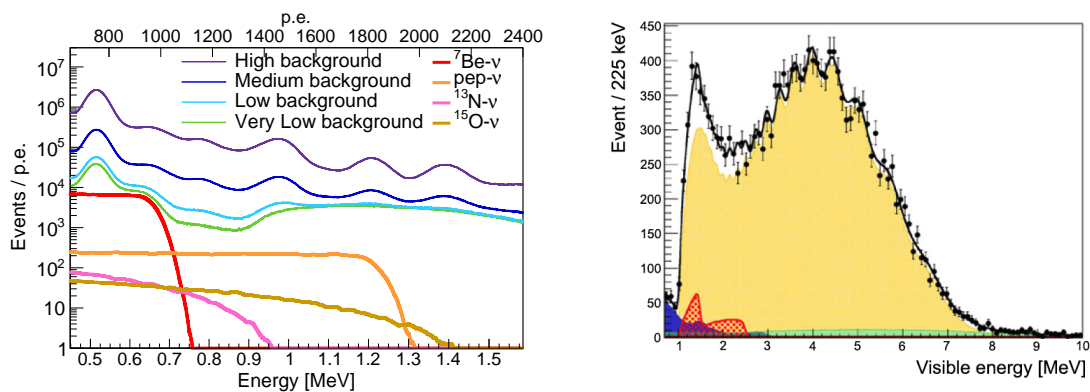


Figure 5. Left: various radiopurity scenarios considered in the JUNO solar neutrino sensitivity study compared to the expected energy spectra of ${}^7\text{Be}$, pep , ${}^{13}\text{N}$, and ${}^{15}\text{O}$ solar neutrinos for one year of statistics. A subtraction of the cosmogenic ${}^{11}\text{C}$ background with the Three-Fold-Coincidence technique is assumed. The top scale is in the number of photoelectrons (p.e.). Right: expected IBD-like spectrum of JUNO for one year of statistics [10]. The respective contributions of geoneutrinos, reactor antineutrinos, accidental background, and cosmogenic ${}^9\text{Li}$ - ${}^8\text{He}$ background are shown in red, yellow, blue, and green, respectively.

3.3. Geoneutrinos

Geoneutrinos are antineutrinos from the decay of long-lived radioactive elements inside the Earth, and can be exploited as a new and unique tool to study our planet, in particular the amount of the Earth's radiogenic heat. Geoneutrinos are detected through the same IBD interaction as the reactor antineutrinos discussed above. The 1.806 MeV kinematic threshold allows for measurement of the high-energy part of geoneutrinos emitted along the ${}^{238}\text{U}$ and ${}^{232}\text{Th}$ chains, while ${}^{40}\text{K}$ geoneutrinos are completely unreachable with the present-day technology. The simulated JUNO IBD-like spectrum for one year of statistics is shown in Figure 5 (Right), with 400 expected geoneutrino events shown in red. JUNO will reach the precision of the current Borexino [19] and KamLAND [20] measurements in about one year [10,21]. Additionally, JUNO will be able to measure the U/Th ratio, a parameter that will provide insights about the Earth's formation processes. Geological study of the local crust is ongoing to facilitate disentangling of the mantle signal and the crustal signal [22,23].

3.4. Supernovae Neutrinos

A core-collapse supernova emits about 99% of its energy via neutrinos. In the few seconds covering the burst, accretion, and cooling stages, an enormous flux of neutrinos of all flavours and electron-flavour anti-neutrinos is emitted. With its large target mass, low energy threshold, and dedicated data acquisition system, JUNO will be sensitive to all flavors of supernova neutrinos through different detection channels [1,10]. For a typical core-collapse supernova at 10 kpc, JUNO will detect thousands of MeV-scale neutrino events. The dominant channel is the IBD interaction, followed by scattering off protons and electrons, then NC and CC interactions on ${}^{12}\text{C}$. About three core-collapse supernova explosions are expected to occur in our galaxy each century. Additionally, a dedicated multi-messenger trigger system will be built to provide a supernovae alert for a global network involving various experiments.

Diffuse supernova neutrino background (DSNB) neutrinos represent an integrated neutrino flux from the past supernova explosions in the visible universe. The DSNB has not been detected yet. JUNO has a large discovery potential of 3σ in three years of data collection for the nominal theoretical SN models [24], as shown in Figure 6 (left). The detection channel is the IBD interaction, which is exploited above the end-point of the reactor antineutrino spectrum at around 10 MeV. Here, the main background will be represented by the NC interactions of atmospheric neutrinos, the influence of which can be

strongly suppressed by a dedicated pulse-shape discrimination technique. The expected signal-to-background ratio of 3.5 could be reached assuming a DSNB signal of a few IBD events per year.

3.5. Atmospheric Neutrinos

As a large target liquid scintillator detector, JUNO will play a major role in the detection of GeV-scale atmospheric neutrinos. The MeV energy scale will be investigated as well, providing a unique benchmark for theoretical models. JUNO will detect atmospheric neutrinos via CC and NC interactions, with the analysis focused on the fully contained CC events [25]. Electron and muon flavour discrimination will be possible by exploiting different hit time pattern. Figure 6 (right) shows the expected performance of JUNO’s reconstruction of atmospheric neutrino energy spectra. A precision of 25% can be achieved with five years of data. Additionally, the θ_{23} mixing angle will be measured with a precision of 6 degrees. By exploiting the effect of matter on neutrino oscillations, atmospheric neutrinos crossing the Earth will provide a complementary sensitivity to NMO that is fully independent of reactor antineutrinos. A combined analysis of reactor and atmospheric neutrinos will further improve the sensitivity of JUNO to NMO.

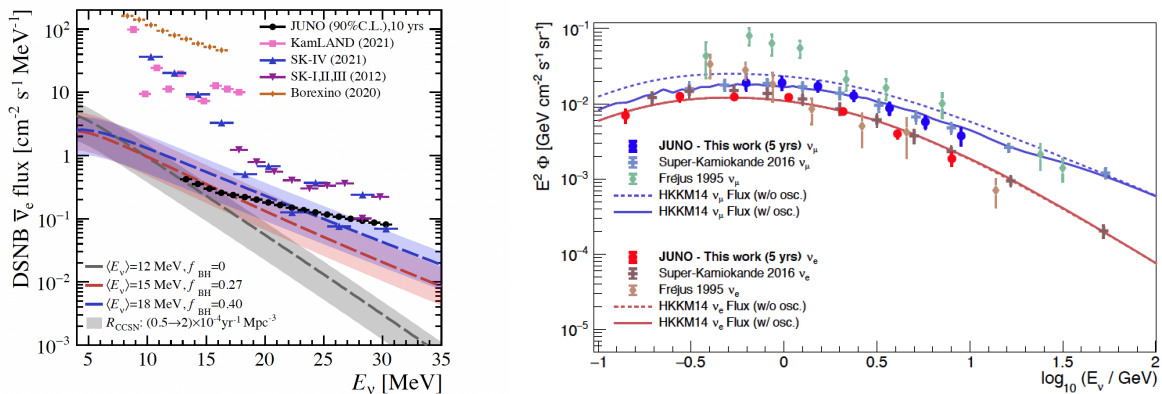


Figure 6. Left: Comparison of model predictions (coloured bands) and existing experimental 90% confidence level upper limits (coloured markers) for the DSNB signal. The estimated sensitivity of JUNO (black markers) reaches the level of current model predictions. From [24]. Right: JUNO’s expected reconstruction of the energy spectra of atmospheric neutrinos of ν_μ (blue) and ν_e (red) flavour [25] with five years of data as compared with existing measurements in the same energy region. The fluxes are multiplied by E^2 for graphical reasons. From [1].

4. Summary and Outlook

Construction of JUNO is currently proceeding, and will be completed by the end of 2023. JUNO’s sensitivity to NMO is 3σ after roughly six years with 26.6 GW_{th} reactor power. In addition to its main goal, JUNO has the potential to study additional neutrino properties and exploit neutrinos as messengers from various astronomical objects, such as the sun, earth, and supernova explosions.

Funding: This work was supported by the Chinese Academy of Sciences, the National Key R&D Program of China, the CAS Center for Excellence in Particle Physics, Wuyi University, the Tsung-Dao Lee Institute of Shanghai Jiao Tong University in China, the Institut National de Physique Nucléaire et de Physique de Particules (IN2P3) in France, the Istituto Nazionale di Fisica Nucleare (INFN) in Italy, the Italian–Chinese collaborative research program MAECI-NSFC, the Fond de la Recherche Scientifique (F.R.S-FNRS) and FWO under the “Excellence of Science—EOS” in Belgium, the Conselho Nacional de Desenvolvimento Científico e Tecnológico in Brazil, the Agencia Nacional de Investigacion y Desarrollo in Chile, the Charles University Research Centre and the Ministry of Education, Youth, and Sports in the Czech Republic, the Deutsche Forschungsgemeinschaft (DFG), the Helmholtz Association and its recruitment initiative and the Cluster of Excellence PRISMA+ in

Germany, the Joint Institute of Nuclear Research (JINR) and Lomonosov Moscow State University in Russia, the joint Russian Science Foundation (RSF) and National Natural Science Foundation of China (NSFC) research program, the MOST and MOE in Taiwan, the Chulalongkorn University and Suranaree University of Technology in Thailand, and the University of California at Irvine in the USA.

Institutional Review Board Statement: Not applicable.

Informed Consent Statement: Not applicable.

Data Availability Statement: Not applicable.

Acknowledgments: We are grateful for the ongoing cooperation from the China General Nuclear Power Group.

Conflicts of Interest: The authors declare no conflict of interest.

References

- Abusleme, A. et al. [JUNO Collaboration]. JUNO physics and detector. *Prog. Part. Nucl. Phys.* **2022**, *123*, 103927. [[CrossRef](#)]
- He, M. et al. [JUNO Collaboration]. Sub-percent Precision Measurement of Neutrino Oscillation Parameters with JUNO. *Chin. Phys. C* **2022**, *46*, 123001. [[CrossRef](#)]
- Strumia, A. and Vissani, F. Precise quasielastic neutrino/nucleon cross-section. *Phys. Lett. B* **2003**, *564*, 42. [[CrossRef](#)]
- Petcov, S.T.; Piai, M. The LMA MSW Solution of the Solar Neutrino Problem, Inverted Neutrino Mass Hierarchy and Reactor Neutrino Experiments. *Phys. Lett. B* **2002**, *533*, 94. [[CrossRef](#)]
- Abusleme, A. et al. [JUNO Collaboration]. Radioactivity control strategy for the JUNO detector. *J. High Energy Phys.* **2021**, *11*, 102.
- Abusleme, A. et al. [JUNO Collaboration]. Optimization of the JUNO liquid scintillator composition using a Daya Bay antineutrino detector. *Nucl. Instr. Meth. A* **2020**, *988*, 164823.
- Abusleme, A. et al. [JUNO Collaboration]. Calibration strategy of the JUNO experiment. *J. High Energy Phys.* **2021**, *3*, 4.
- Abusleme, A. et al. [JUNO Collaboration]. TAO Conceptual Design Report: A Precision Measurement of the Reactor Antineutrino Spectrum with Sub-percent Energy Resolution. *arXiv* **2020**, arXiv:2005.08745.
- Abusleme, A. et al. [JUNO Collaboration]. The Design and Sensitivity of JUNO's scintillator radiopurity pre-detector OSIRIS. *Eur. Phys. J.* **2021**, *81*, 973. [[CrossRef](#)]
- An, F. et al. [JUNO Collaboration]. Neutrino physics with JUNO. *J. Phys. G Nucl. Part. Phys.* **2016**, *43*, 030401. [[CrossRef](#)]
- Abusleme, A. et al. [JUNO Collaboration]. Mass Testing and Characterization of 20-inch PMTs for JUNO. *Eur. Phys. J. C* **2022**, *accepted for publication*.
- Wang, Y. et al. A new optical model for photomultiplier tubes. *Eur. Phys. J. C* **2022**, *82*, 329. [[CrossRef](#)]
- Abusleme, A. et al. [JUNO Collaboration]. Feasibility and physics potential of detecting ^8B solar neutrinos at JUNO. *Chin. Phys. C* **2021**, *45*, 023004. [[CrossRef](#)]
- Zhao, J. et al. [JUNO Collaboration]. Model Independent Approach of the JUNO ^8B Solar Neutrino Program. *Astrop. Phys. J.* **2022**, *submitted publication*.
- Abusleme, A. et al. [JUNO Collaboration]. JUNO sensitivity to ^7Be , *pep*, and CNO solar neutrinos. *J. Cosm. Astrop. Phys.* **2023**, *accepted publication*.
- Agostini, M. et al. [Borexino Collaboration]. Experimental evidence of neutrinos produced in the CNO fusion cycle in the Sun. *Nature* **2020**, *587*, 577. [[CrossRef](#)]
- Agostini, M. et al. [Borexino Collaboration]. Comprehensive measurement of pp-chain solar neutrinos. *Nature* **2018**, *562*, 505. [[CrossRef](#)]
- Appel, S. et al. [Borexino Collaboration]. Improved measurement of solar neutrinos from the Carbon-Nitrogen-Oxygen cycle by Borexino and its implications for the Standard Solar Model. *Phys. Rev. Lett.* **2022**, *accepted for publication*.
- Agostini, et al. [Borexino Collaboration]. Comprehensive geoneutrino analysis with Borexino. *Phys. Rev. D* **2020**, *101*, 012009. [[CrossRef](#)]
- Abe, S. et al. [KamLAND Collaboration]. Abundances of Uranium and Thorium Elements in Earth Estimated by Geoneutrino Spectroscopy. *Geophys. Res. Lett.* **2022**, *49*, e2022GL099566. [[CrossRef](#)]
- Han, R.; Li, Y.F.; Zhan, L.; McDonough, W.F.; Cao, J.; Ludhova, L. Potential of geo-neutrino measurements at JUNO. *Chin. Phys. C* **2016**, *40*, 033003. [[CrossRef](#)]
- Reguzzoni, M.; Rossi, L.; Baldoncini, M.; Callegari, I.; Poli, P.; Sampietro, D.; Strati, V.; Mantovani, F.; Andronico, G.; Antonelli, V.; et al. GIGJ: A crustal gravity model of the Guangdong Province for predicting the geoneutrino signal at the JUNO experiment. *J. Geophys. Res. Solid Earth* **2019**, *124*, 4, 4231. [[CrossRef](#)]
- Gao, R. et al. JULOC: A local 3-D high-resolution crustal model in South China for forecasting geoneutrino measurements at JUNO. *Phys. Earth Planet. Inter.* **2020**, *299*, 106409. [[CrossRef](#)]

24. Abusleme, A. et al. [JUNO Collaboration]. Prospects for Detecting the Diffuse Supernova Neutrino Background with JUNO. *J. Cosmol. Astropart. Phys.* **2022**, *10*, 33.
25. Abusleme, A. et al. [JUNO Collaboration]. JUNO sensitivity to low energy atmospheric neutrino spectra. *Eur. Phys. J. C* **2021**, *81*, 887. [[CrossRef](#)]

Disclaimer/Publisher's Note: The statements, opinions and data contained in all publications are solely those of the individual author(s) and contributor(s) and not of MDPI and/or the editor(s). MDPI and/or the editor(s) disclaim responsibility for any injury to people or property resulting from any ideas, methods, instructions or products referred to in the content.